Positronium Annihilation Lifetime Spectroscopy Study of SBA-15

Tracy K. Steinbach
Grand Valley State University

April 22, 2010

Abstract

Positronium annihilation lifetime spectroscopy (PALS) is a technique used in the characterization of porosity in nanostructured materials. Positrons, the antiparticle to the electron, enter a sample and either immediately annihilate with an electron or they can capture an electron to form Positronium (Ps), the hydrogen-like bound state. Ps then annihilates with a lifetime corresponding to the pore size. This annihilation converts the total mass of the positron and electron into high-energy photons. These annihilations are detected to measure Positronium lifetime. SBA-15, a mesoporous silica that consists of a two dimensional hexagonal array of cylindrical mesopores with interconnecting micropores, is a system of interest as a catalysis support and low-dielectric constant material. Nitrogen adsorption, x-ray diffraction, and small angle neutron scattering (SANS) have been used to characterize the pore structure in SBA-15, but none of these techniques have been able to yield a complete picture. PALS is a technique that has the potential to yield insight of the pore structure in SBA-15.

1 Introduction

The porosity of a material is the volume within a substance *not* taken up by the material itself, i.e. the free volume. The porosity plays a key role in determining a material's macroscopic physical properties. In polymers, the porosity of the polymer plays a key role in the mechanical, electrical, and transport properties. For example, one specific physical property of polymers defined by the free volume is the glass transition temperature. This is the temperature at which a polymer transitions between a "glassy" phase where the mobility of the polymer chains is highly frustrated and the "rubber" phase where they are highly mobile and able to relax to equilibrium. For example, at room temperature, the polymer in your eye glasses is in the glassy phase while saran wrap is in the rubber phase. Porosity also plays a major role in determining many important properties of porous low dielectric constant (low-k) materials. The density, stiffness/strength, thermal conductivity, and chemical reactivity of a dielectric material all depend in part on its porosity [3].

A material that falls in the latter category is a particular composition of mesoporous silica called Santa Barbara A 15 (SBA-15). SBA-15 is made up of a two dimensional hexagonal array of cylindrical mesopores with interconnecting micropores, as shown schematically in Figure 1. By varying the temperature and time used to synthesize SBA-15, the wall thickness and pore radius can be varied. The typical pore diameters seen for SBA-15 range from 3 to 30 nm [8]. There are many applications for which SBA-15 may be applied, including but not limited to catalysis support, low-k dielectric, gas adsorption, and drug delivery [4].

An application of SBA-15 is for use as a low-k dielectric material. As the porosity of a material increases, the dielectric constant is driven down from that of the base material, making the material useful in microelectronics among other applications. The lower dielectric constant materials help increase the complexity of computer chips, while at the same time minimizing the size of the chip, and improving circuit speed and memory capacity within

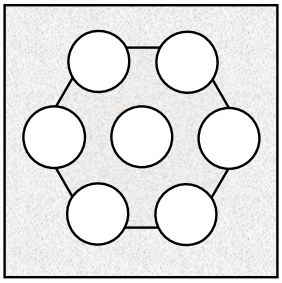

Figure 1: Schematic drawing of SBA-15. SBA-15 consists of a two dimensional hexagonal array of cylindrical mesopores with interconnecting micropores.

computers and other electronic devices [3].

One area of active research is in the use of SBA-15 as a catalysis support in Fischer-Tropsch synthesis, which is being studied by a group from the University of Maine [6]. Fischer-Tropsch synthesis is a catalyzed chemical reaction through which hydrocarbon fuels are produced from carbon monoxide and hydrogen. The reaction requires the use of catalysts such as iron, cobalt, nickel, or ruthenium to produce synthetic fuels. SBA-15 can be used as a catalysis support to balance metal dispersion in the reaction as well as limiting the transportation of reactants (CO and H_2) into the reaction and the products (normally alkanes) out of the reaction.

To be able to take full advantage of SBA-15 in any application, the details of the pore structure must be better understood. The pore structure of SBA-15 has been previously studied using several metrologies, including small angle neutron scattering (SANS) and small angle x-ray scattering (SAXS). The techniques have proposed a model for the structure of SBA-15, as shown in Figure 1 [12]. However, these techniques have limitations that may have yielded an incomplete model for the structure of SBA-15.

SANS measures the momentum transfer that occurs when neutrons pass through a sample. In SANS we are only concerned with elastic scattering (no energy change of the neutron)

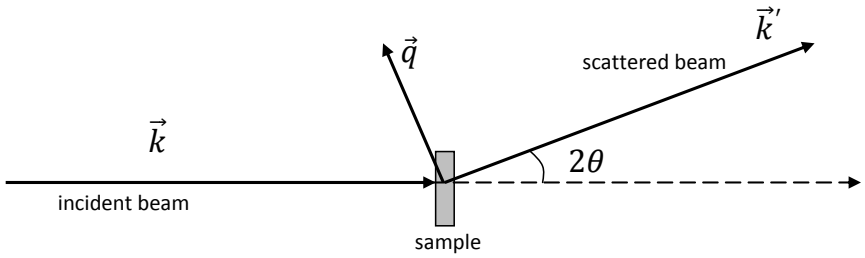

Figure 2: Small angle neutron scattering momentum transfer diagram.

and so the incident momentum vector, $\vec{k}$, and the neutron's scattered momentum vector, $\vec{k}'$, are equal in magnitude. However, there is a change in direction, with θ as the scattering angle, due to the inhomogeneities in the sample. Because the neutron also acts as a wave, we can write the magnitude of the momentum as $p = mv = \hbar k = 2\pi\hbar/\lambda$, and the magnitude of the momentum transfer (also known as the scattering angle) $\vec{q} = \vec{k}' - \vec{k}$ is given as

$$q = |\vec{k}' - \vec{k}| = \frac{4\pi \sin\theta}{\lambda}$$

where m is the neutron mass, v is the speed of the neutron, and λ is the wavelength. From Bragg's law, $n\lambda = 2d\sin\theta$, with n being the order of the reflection and d being the spacing between lattice planes, we can find the location of scattering peaks from the constructive interference of wave interacting with periodic structures [11].

Through these methods SANS has provided some very important information about the structure of SBA-15, but it has its limitations. One major limitation encountered in SANS is that the results found using SANS are very model-dependent when converting from the scattering angle to the pore size. If the model used in analyzing the scattering angle does not match completely with the actual structure of the pores the final results may be inaccurate. Additionally, SANS frequently requires the use of a solvent (typically H_2O, D_2O, or a mixture of both) in order to provide contrast matching of certain areas of the sample.

Contrast matching is used to mask the scattering signal from certain parts of a sample, so that the signals from other parts of the sample can be seen more clearly. However, many samples do not retain their original pore structure when a solvent is added, thus causing SANS to produce results that may not completely match the pore structure actually present in the sample.

Positronium annihilation lifetime spectroscopy (PALS) is a metrology that has been used to study porous materials for several decades [7] and is a complementary technique that could yield additional insight about the pore structure of SBA-15. Details on the PALS technique will be presented shortly. In contrast to SANS, PALS is much less model-dependent and does not require a solvent, thus it should give complementary results about the structure of SBA-15. Another advantage of PALS is that it requires smaller scale equipment compared to SANS (the PALS instrumentation can be set up on a bench top).

2 Background Theory

PALS is an experimental technique that utilizes antimatter, namely the positron. The positron, the antiparticle to the electron, is produced in two different ways. Positrons can either be emitted in radioactive decay of certain nuclei, including ^{22}Na, ^{58}Co, ^{64}Cu, and ^{68}Ge (which is convenient for use in a research lab), or are formed through pair production. Pair production occurs when a high-energy γ-ray having energy greater than 1022 keV interacts with a heavy nucleus to convert energy into mass and produce a positron and an electron (as well as a photon that is absorbed into the nucleus to conserve momentum). Pair production is essentially the reverse process of positron/electron annihilation.

When a positron enters a material it will eventually annihilate with an electron. This annihilation converts the total mass, m, of the positron and the electron into energy, E,

in the form of high-energy photons. This conversion of mass into energy, in the form of photons, follows Einstein's equation, $E = mc^2$. In many cases the positron and electron do not immediately annihilate; instead they may first form the hydrogen-like bound state of a positron known as positronium (Ps). The time from when Ps is formed until it annihilates is known as its *lifetime*. The lifetime of Ps is dependent upon the environment in which it is found, as well as its state.

Positronium has two states, singlet (*para*-) and triplet (*ortho*-), that are dependent upon the relative spin state of the positron and electron. *Para*-Ps has a spin state of 0, while *ortho*-Ps has a relative spin state of 1. The annihilation of *para*-Ps occurs with the emission of two back-to-back γ-rays of 511 keV, with a short vacuum lifetime of $\sim$125 ps [7]. This is a 2γ annihilation that conserves both momentum and energy. To conserve angular momentum and charge conjugation *ortho*-Ps is required to annihilate into at least three photons (3γ annihilation). *Ortho*-Ps has an odd charge conjugation, as do photons, so when *ortho*-Ps annihilates it must annihilate into an odd number of photons; to conserve momentum it must annihilate into at least three photons [10]. The lifetime of *ortho*-Ps in vacuum is $\sim$142 ns [7].

These characteristic lifetimes for *para*- and *ortho*-Ps are dependent upon the environment surrounding the Ps. This dependence is the driving principle behind the PALS technique, which uses measured lifetimes in a material to discern the structure of porous materials. Once formed, positronium tends to locate within the voids, or pores, in the material where the net Ps energy is the lowest. When positronium is within the pores its energy is low because the electrons in the material are far away. Though Ps locates in the voids of a material, it still interacts with the walls of the pores. The more often it interacts with the material, the more likely it is to annihilate. The measured decay rate, λ_m, is the sum of the

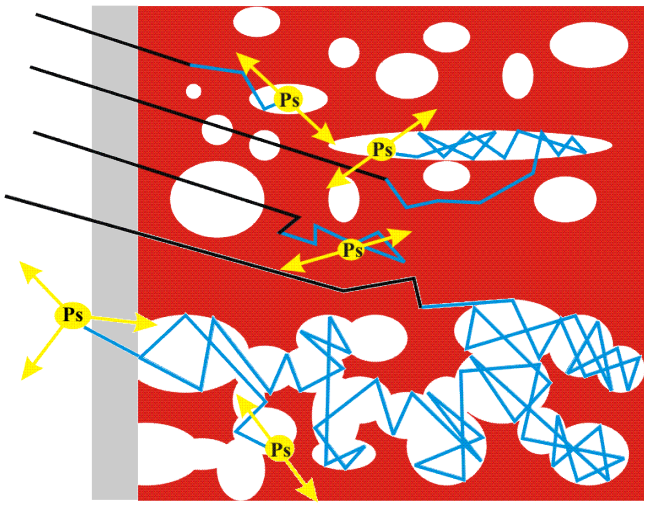

Figure 3: Positronium formation in porous materials. Positrons that enter a sample form Ps, which tends to localize in pores if it does not annihilate immediately. The Ps interacts with the pore walls, shortening its lifetime. From reference [7].

vacuum decay rate, λ_{vac}, plus the quenching rate, λ_{quench}.

$$\lambda_m = \lambda_{vac} + \lambda_{quench}$$

(Note that the decay rate, λ, is inversely proportional to the lifetime, τ.) The smaller a pore is the more the Ps will interact with the walls (quenching) and thus the sooner it will annihilate, yielding a shorter lifetime. Quenching is annihilation with an electron the Ps is not bound to. The idea of this Ps interaction in a material is depicted in Figure 3. By measuring the shortened lifetime of Ps the average pore size can be determined [7].

3 Methods

A schematic of the PALS apparatus used to measure the lifetime of Ps in the material is shown in Figure 4. A sealed ^{22}Na radioactive positron source is embedded in a bulk sample of SBA-15 powder. Two fast plastic scintillators are used to detect γ-rays. The *start detector*

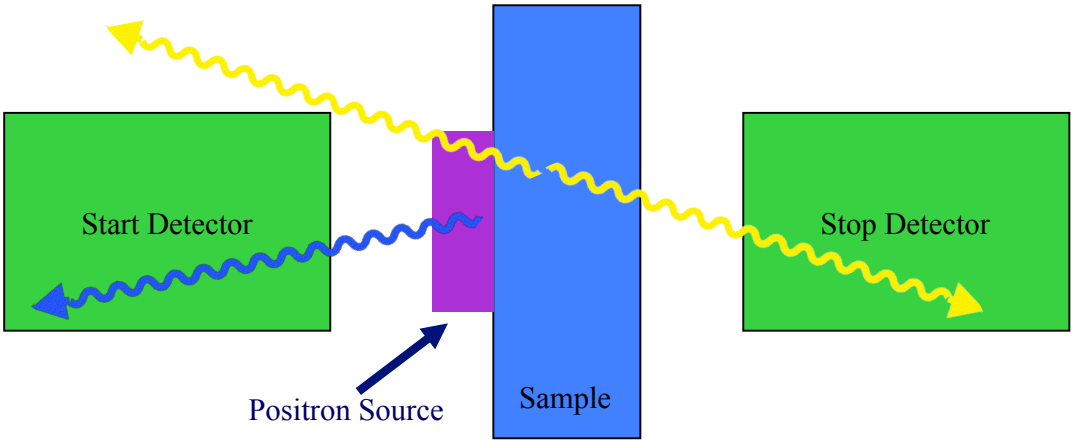

Figure 4: Schematic drawing of PALS apparatus

is setup to be sensitive to the 1270 keV γ-ray emitted concomitantly with the emission of a positron from the ^{22}Na source. These positrons thermalize in the material and form Ps. The *stop detector* is setup to detect the 511 keV annihilation γ-ray. The stop and start pulses are presented to a time to analog converter (TAC). A multichannel analyzer (MCA) is used to record the TAC timing pulse in a computer. This process is repeated many times, and all the lifetimes are used to generate a lifetime histogram similar to the spectra seen in Figure 5. This histogram is then fitted to one or more Ps lifetime(s) and intensity(ies). From these fitted lifetimes the pore diameter(s) within the sample are determined.

The sample cell used, shown in Figure 6, was machined from stock aluminum. A 1" x 1" x .8" aluminum block was machined for the main component of the cell and a 1" x 1" square of sheet aluminum was cut to create a lid. The central hole drilled in the block is designed to hold the ^{22}Na source surrounded by the SBA-15 power (using approximately a cubic centimeter of sample). The lid is screwed to the base of the cell. Due to time constraints we were not able to construct a sample cell that could would allow direct vacuum pumping,

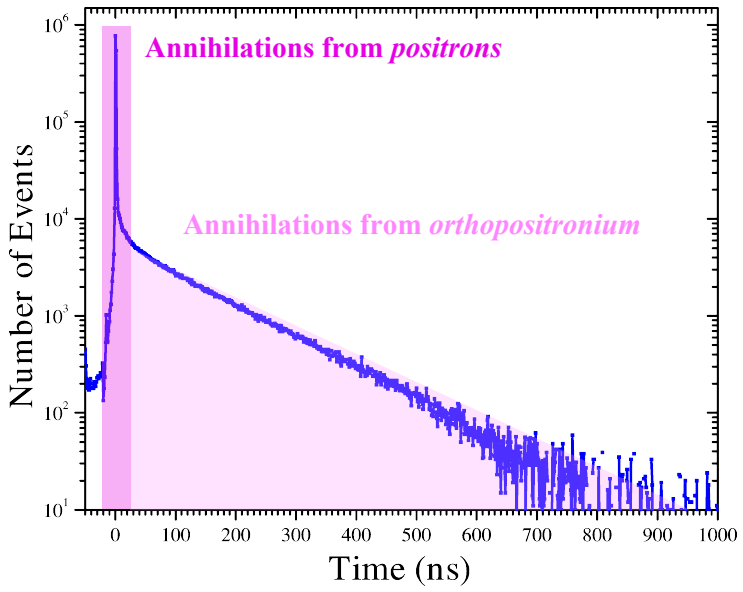

Figure 5: Typical lifetime spectra for Ps in porous material (not SBA-15). Characteristic lifetime, τ, is shortened by Ps quenching. From reference [1].

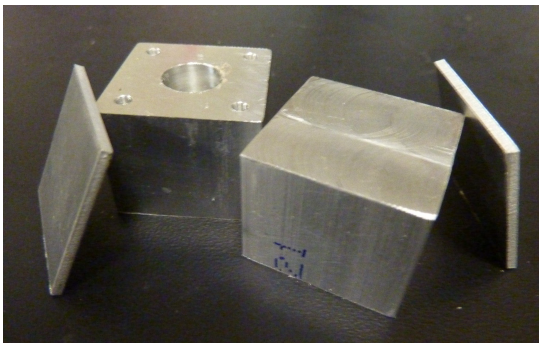

Figure 6: Sample Cell. The sample cell was machined from aluminum to hold the positron source and the sample of SBA-15

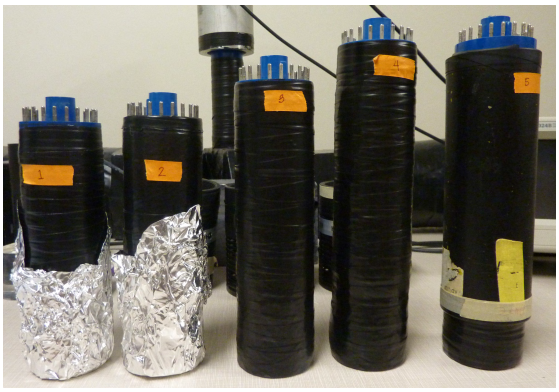

Figure 7: Set of phototubes tested. Phototubes 3 and 4 were used in the final apparatus.

Figure 8: Three of the five bases tested. Bases A and B were used in the final apparatus

instead the sample cell was placed in a desiccator that could be pumped down to a few microns of vacuum. After the desiccator was evacuated the detectors were brought in as close to the cell as possible and data was run.

Photomultiplier tubes are photon detectors that utilize the photoelectric effect. When radiation falls upon a metal surface, electrons are emitted if the photon energy is greater than the work function of the material being irradiated. The work function is the minimum energy needed to remove an electron from an atom. These initial electrons that are emitted are then accelerated from the photocathode into a series of dynodes. Each dynode emits multiple electrons for each one that hits it, increasing the number of electrons after each dynode. [9]

A set of five phototubes (shown in Figure 7) and five bases (shown in part in Figure 8) were tested to determine which worked the best and would then be used in the final apparatus. A block of fast plastic scintillator was milled and polished to use in this testing process. Each phototube was tested with two different bases at three voltages on each base to give a rough view of which phototubes provided the most gain at the lowest voltage input. An example of the pulse output directly from the phototubes is seen in Figure 9. The two

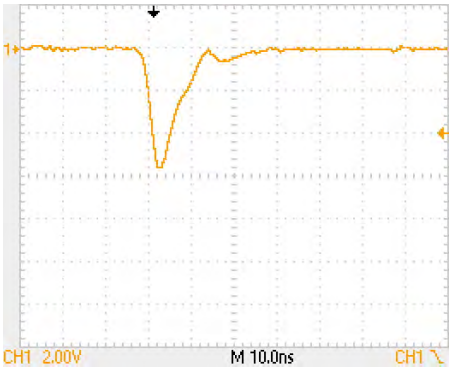

Figure 9: Negative output pulse directly from phototube. The pulse seen here is ~ 5.5V

phototubes that exhibited similar gains over a low voltage input where chosen to use in the final bulk PALS apparatus. One of these phototubes was then used to test all five bases at three input voltages each to find which bases produced the largest peaks for the same voltage inputs. The two bases that gave the best outputs were used in the final apparatus.

Once the best phototubes/bases were found the final detectors were constructed. Two cast fast plastic scintillator cylinders were used in constructing the apparatus detectors. Each plastic scintillator had a two inch diameter to match the dimensions of the phototubes used. Photonis XP2020UR phototubes where used. These phototubes have a two inch diameter and exhibit a gain of 3×10^7, a rise time of 1.4 ns, and a peak wavelength with the range of 400-430 nm. EJ-204 plastic scintillator was used, exhibiting a decay time of 1.8 ns and a peak wavelength of approximately 410nm. This type of scintillator was chosen because its peak wavelength falls within the peak wavelength range of the XP2020UR phototubes used and has a short decay time. The scintillator used for the start detector was two inches thick to stop more of the 1270 keV γ-rays, while the scintillator used for the stop detector was one inch thick due to the reduced need of material to stop the 511 keV γ-rays. The thinner scintillator was paired with the slightly better phototube to adjust for the smaller gain within the scintillator. EJ-550 optical grade silicone grease was used to create an optical

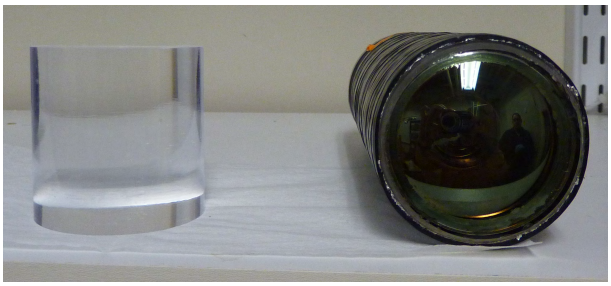

Figure 10: Fast plastic scintillator cylinder and photomultiplier tube.

Figure 11: Wrapped phototubes.

interface between the plastic scintillator and the glass of the phototube. Both the tube and the scintillator were wrapped in aluminum foil, to reflect light from the surface, and then wrapped in black electrical tape, to mechanically hold the two pieces together and block external light. Magnetic shielding made from μ-metal (a high permeability material) was then added to the outside of each phototube to minimize degradation of the output pulse due to stray fields.

The output of the phototube pulse is sent to a discriminator that selects a range of signals that correspond to a photon of interest and outputs a standard NIM pulse to present to the TAC. The start discriminator uses lower level discrimination set to select 1270 keV γ-ray pulses from the start detector. The stop discriminator has both a lower level discriminator and an upper level discriminator. The lower level filters out background noise, while the high end filters out the 1270 keV γ-ray events from the birth of Ps so that the 511 keV pulses are selected. To find where the discrimination levels should be set for both discriminators discriminator curves are constructed, see Figures 12-14 . Discriminator curves are produced by recording the number of counts per second across the entire range of the discriminator. As different slopes appear in the curve, different types of events (background noise, 511 keV γ-rays, and 1270 keV γ-rays) are being filtered out. By finding when the knees (sharp changed in the count rate - shown with arrows in Figure 12-14) occur we can locate the level we want to set the each discriminator to, allowing the best timing.

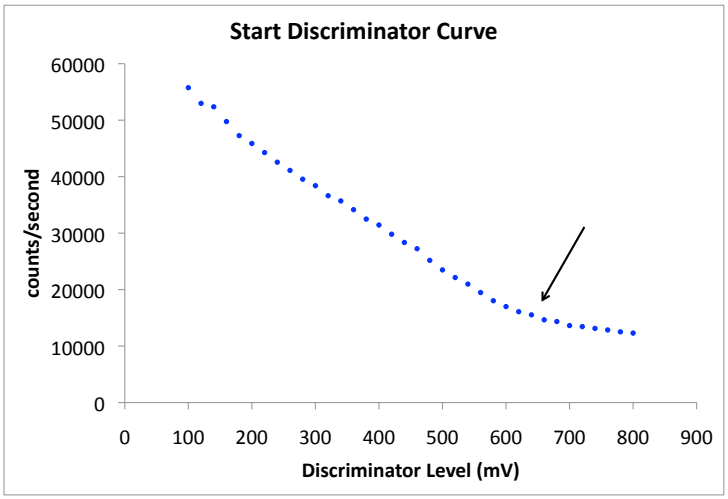

Figure 12: Start discriminator curve. Finds the knee between 1270 keV events and 511 keV events to set the cutoff level for the start discriminator.

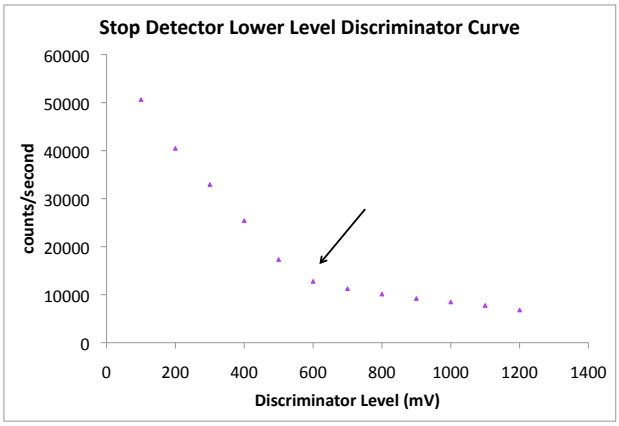

Figure 13: Stop lower level discriminator curve. Finds the knee between the background events and the 511 keV events to set the lower level cutoff for the stop discriminator.

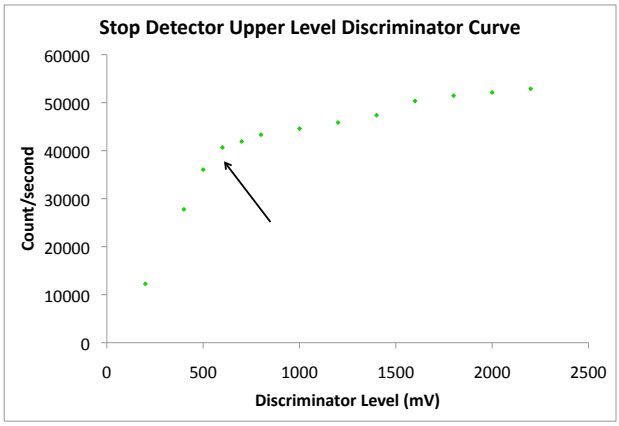

Figure 14: Stop upper level discriminator curve. Finds the knee between the 511 keV events and the 1270 keV events to set the upper level cutoff for the stop discriminator.

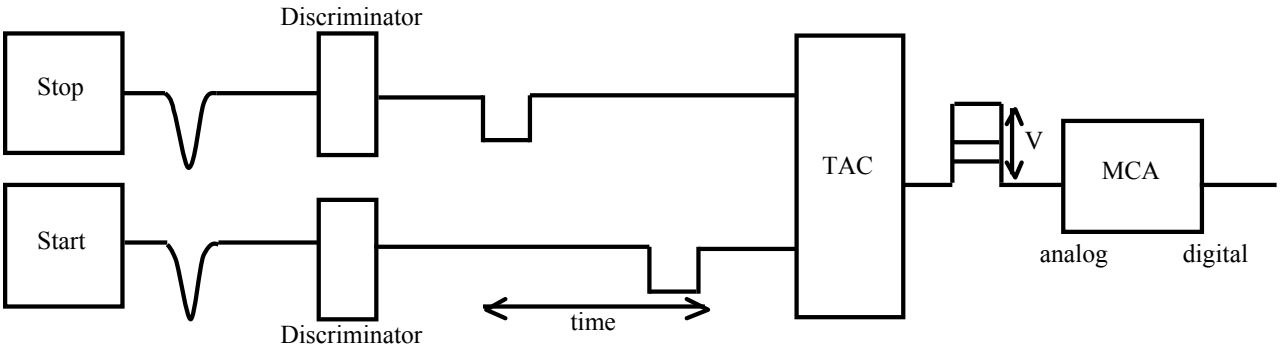

Figure 15: Schematic drawing of timing electronics. The output of the start and stop detectors are sent to discriminators that select the signals of interest from each detector. The discriminator pulses are sent to the TAC to determine the time between start and stop events. The output pulse from the TAC corresponds to this time and is sent to the MCA. The MCA takes this analog signal and converts it to a digital signal.

Start and stop events are presented to the time to analog converter (TAC), which then determines the time difference between the events. The TAC then sends out a square wave pulse, whose height corresponds to the lifetime of the Ps annihilation event seen, to the multi-channel analyzer (MCA). The MCA records the TAC timing pulses and converts the analog signal to a digital one that can then be read and recorded by a computer. A schematic of the time electronics is seen in Figure 15 and the actual timing electronics can be seen in Figure 16. This process of recording a single event is repeated many times to generate a lifetime histogram, an example of such a histogram is seen in Figure 17. The dead time, or the amount of time during which we are unable to process another signal, sets the rate at which data can be taken. The time from when start is triggered until when the data is stored and the detector reset is approximately 2 μs, allowing 500,000 events per second.

These lifetime histograms consist of several pieces (as labeled in Figure 17). The first, occuring at short times, is the prompt peak. This peak is due to events that are either direct annihilation or the annihilation of *para*-Ps. The second piece is the lifetime (or lifetimes) of

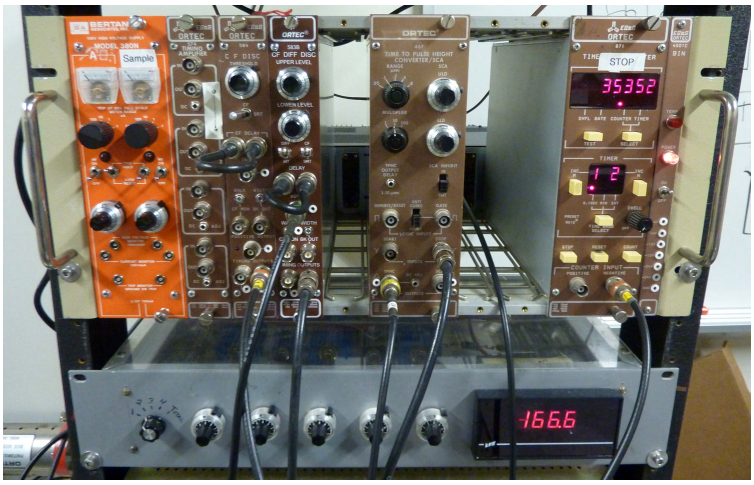

Figure 16: Timing electronics. Starting from top right we have the counter that was used to construct the discriminator curves, the TAC, the stop discriminator, and the start discriminator (the last two modules were not used in our timing electronics).

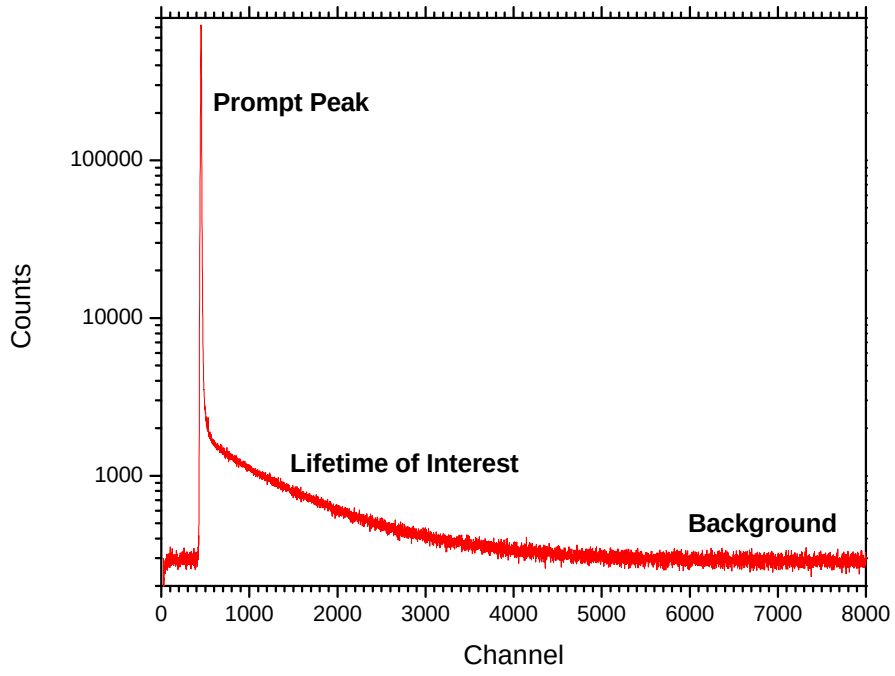

Figure 17: Evacuated SBA-15 raw data. Raw data from evacuated SBA-15; not background subtracted. Time per channel is approximately 100 ps

interest (due to the quenching of *ortho*-Ps) that decay exponentially. The final piece is the flat background due to random events. For an ideal spectrum the number of decays at a particular time after $t = 0$ (identified as the center of the prompt peak) is given by

$$\mathrm{N}(t) = \mathrm{A}e^{-\lambda t} + \mathrm{B}$$

where A is the intensity of a component with a decay rate λ, and B is the background. We use a program called PAScual [2] that is designed to fit the full spectrum to extract the lifetimes and intensities of any decay components. The lifetime can be converted into a pore diameter using a standard model of Ps annihilation in pores [5],[7].

4 Results and Discussion

After setting up and testing the bulk PALS system we have achieved preliminary results of SBA-15 in air and evacuated SBA-15. Data was first taken in air, the detectors were placed directly against the side of the cell to maximize detection efficiency of the 1270 kev and annihilation γ-rays. The setup was run for 18 hours. The resulting spectra are the blue curves in Figures 18 and 19. Note that the spectra have had the background subtracted and they have been normalized to the total counts in the spectrum. This was done to make comparison between spectra straight forward. When fit, this data yielded a lifetime of ~ 58 ns. Which is consistent with Ps annihilation in air.

After the system was run in air the sample was placed in the vacuum desiccator to allow the sample to be evacuated. In this case the detectors were brought up to the side of the desiccator (as close as possible but not directly in contact with the sample cell as when the system was run in air). A comparable amount of data (to that taken in air) was aquired in 24 hours. As can be seen in Figure 18 the evacuated SBA-15 (red curve) exhibits a

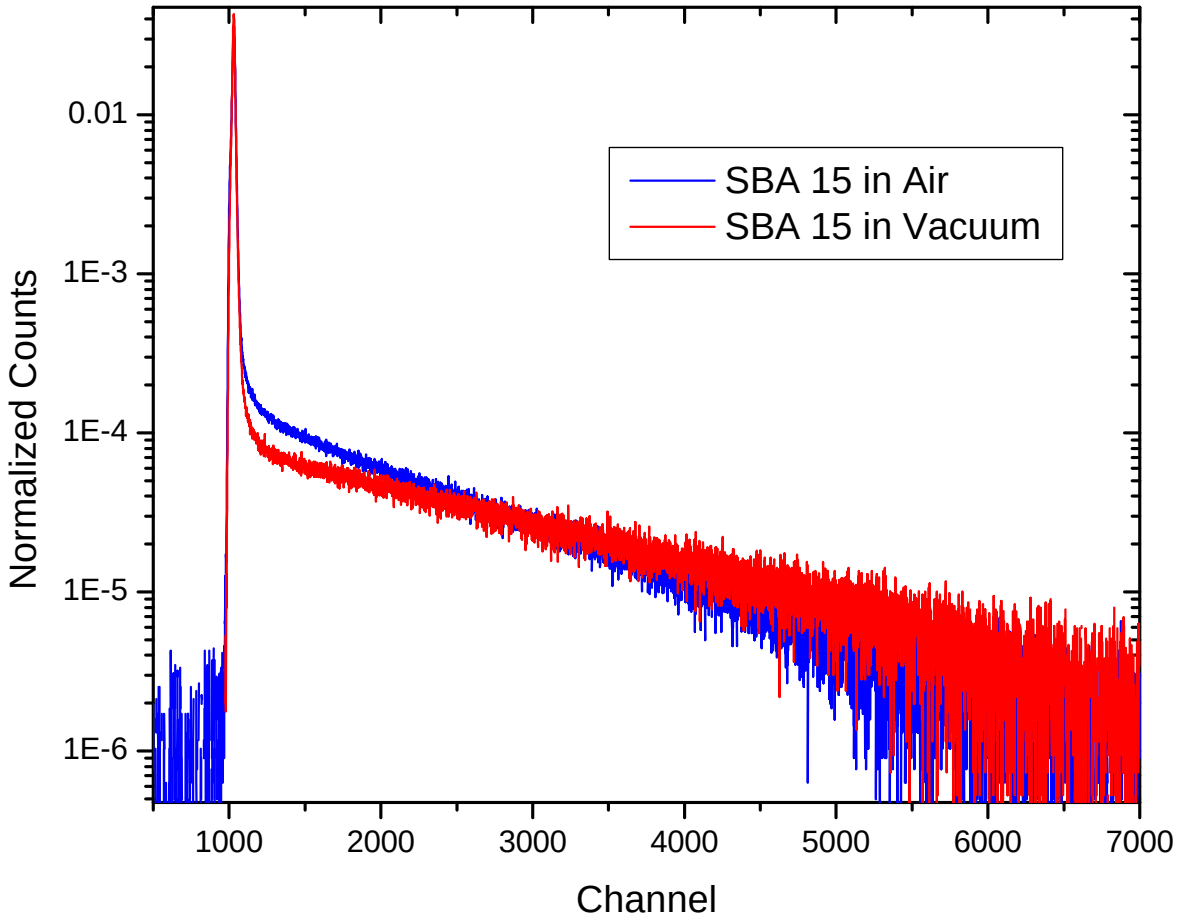

Figure 18: SBA-15 data in air (blue curve) and evacuated (red curve). The spectra have had the background subtracted and have been normalized to the total counts in the spectrum. As can be seen here the evacuated sample exhibits a longer lifetime than SBA-15 in air.

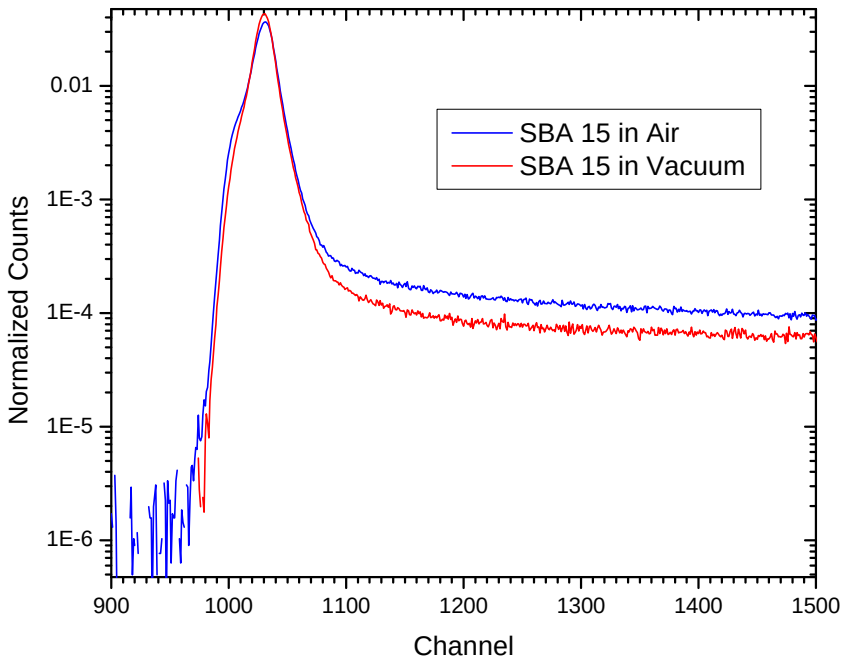

Figure 19: Air and evacuated SBA-15 data zoomed in on the prompt peak and short time region. Time per channel is approximately 50 ps

longer lifetime than that of SBA-15 in air (i.e. it does not decay as quickly as seen with the air filled sample). The fit yielded a lifetime of the evacuated SBA-15 of $\sim$ 65 ns. This lifetime correlates to an average pore diameter of 5.0-5.5 nm, which is consistent with what we expected to see for the mesopores of SBA-15.

As mentioned a longer lifetime was seen for evacuated SBA-15 compared to the sample in air. This result is an expected one because the air filled pores contain oxygen which is known to have an unusually high quenching rate of Ps. The presence of oxygen should shorten the lifetime seen in an evacuated sample, which we have seen. Though we are clearly seeing a difference between the lifetime in air filled pores and evacuated pores we cannot be certain if we were able to fully evacuate the pores. If there was still some air in the pores the lifetime found from the current data may not be the real lifetime of Ps in fully evacuated SBA-15. Thus, the pores in the sample may be even *larger* than what we are measuring.

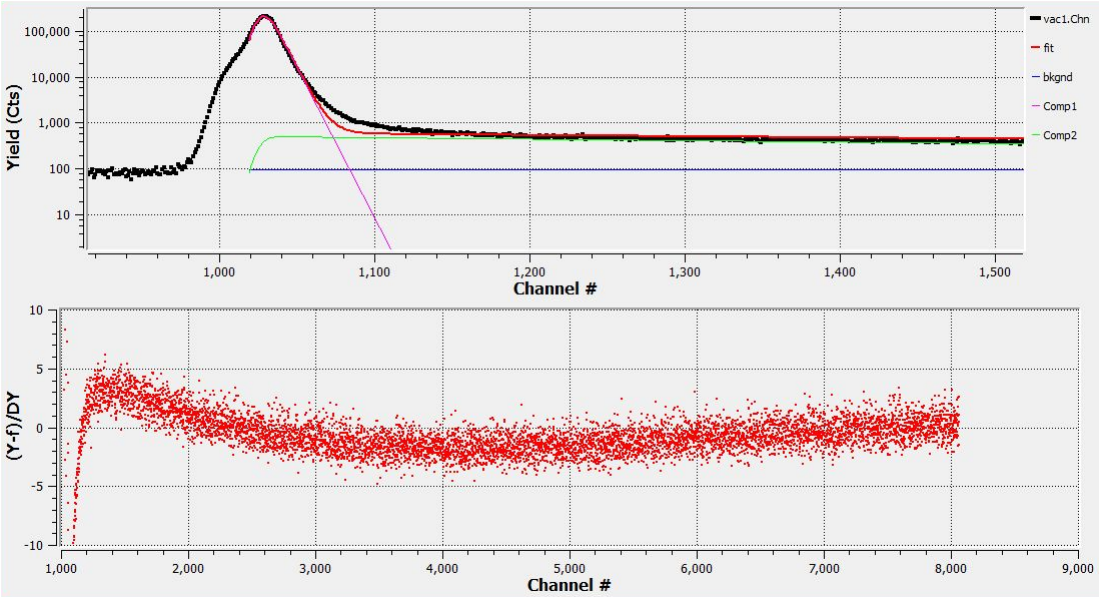

Figure 20: Raw data and spectrum fit. In the top graph the black data points is the raw data. The green line is that fit to the lifetime of interest. The magenta line is that fit to the prompt peak and the blue line is the background fit. The red line is the total fitted spectrum. The bottom plot is the residual between the raw data and the fit.

Though our preliminary data seems to fit with what we were expecting to see for the mesopores, there seems to be a lifetime (possibly from the micropores - pores less than 1 nm in diameter - within the sample) that is not currently being fit. This can be seen in Figure 20, where the fitted spectrum does not match the data in the short time range after the prompt peak. This is clearly evident in the residual plot where the fitted value is lower than the actual data. It is in this region that we believe there is another lifetime due to the micropore structure in the matrix material of SBA-15.

5 Conclusion

We succeeded in building a bulk PALS systems and using it to make preliminarily measurements of the Ps lifetime in both evacuated SBA-15 and SBA-15 in air, giving us a good estimate of the average pore diameter of the mesopores within the sample. From here, there

is much more work that can be done. First we need to take more data in general. Due to complications we were not able to run as much as planned and so do not have as much data as we would like.

We would also like to run in a better vacuum system. Due to time constraints, the evacuated data seen in Figures 18 and 19 was collected using a vacuum pumped desiccator rather than the vacuum system hooked up directly to the sample cell as planed. This setup drastically lowered the detection efficiency and required that we run longer to achieve reasonable statistics. To build this vacuum pump-able sample cell we plan to utilize a cell similar to the one we used with some modifications. Between the lid and base of the cell a rubber gasket will be placed to allow for a good seal. A filter that traps particles larger than 0.5 μm is inserted through the side of the cell to allow the sample to be vacuum pumped without the small grains of the sample being pumped out. The start and stop detectors would then be brought in from the top and bottom of the cell to minimize the amount of aluminum between the sample and the detectors to optimize the efficiency.

To uncover the lifetime of the micropores from that of the mesopores we would like to back fill the sample with a gas such as N_2 (a gas that has a known Ps lifetime). The hopes is that this would essentially force Ps to annihilate in the micropores by preventing diffusion from the micropores into the much larger mesopores. Since the Ps lifetime in N_2 is known it can be accounted for. We hope that this would allow us to gain a better insight of how these micropores interconnect throughout the material which is of interest to the group from the University of Maine.

Acknowledgements

I would like to thank my advisor, Dr. Richard Vallery, for all of his help and guidance with my project. I would also like to thank Rachel Pollock from the University of Maine for

the sample of SBA-15 and the help she has given me in finding information for my project. I would also like to thank Dave Gidley from the University of Michigan for all of the equipment he has provided me with for my project. The physics department at Hope College is also due thanks for the use of their TAC after ours died. A lot of thanks also goes to the physics department at Grand Valley State University for their support of my research.

References

[1] Private communication with R. Vallery.

[2] PAScual data analysis software see http://sourceforge.net/apps/mediawiki/pascual/index.php?title=FAQ.

[3] Baklananov, M., Green, M., and Maex, K. *Dielectric Films for Advanced Microelectronics*. John Wiley Sons Ltd., West Sussex, England (2007).

[4] Bhattacharya, S., Casne, B., Hung, F.R., and Gubbins, K.E. *Modeling Micelle-Templated Mesoporous Material SBA-15: Atomistic Model and Gas Adsorption Studies*. In Langmuir (2009).

[5] Dull, T., Frieze, W., Gidley, D.W., Sun, J., and Yee, A. *Determination of Pore Size in Mesoporous Thin Films from the Annihilation Lifetime of Positronium*. In J. Phys. Chem., (105) (2001).

[6] Frederick, B., Pollock, R., and Melnichenko, Y. *Pore Accessibility in Mesoporous Silica using CM-SANS*. In (2008).

[7] Gidley, D.W., Peng, H.G., and Vallery, R.S. *Positron Annihilation as a Method to Characterize Porous Materials*. In Reviews in Advance (2006).

[8] Imperor-Clerc, M. and Davidson, P. *Existence of a Microporous Corona around the Mesopores of Silica-Based SBA-15 Materials Templated by Triblock Copolymers*. In J. Am. Chem. Soc. (2000).

[9] Moore, J.H. and Davis, C.C. *Building Scientific Apparatus*. Cambridge University Press, Cambridge (2009).

[10] Nico, J.S. *Precision Measurement of the Orthopositronium Decay Rate Using the Vacuum Technique* (1991).

[11] Remmes, N. *Design of the Small Angle Neutron Scattering Instrument at the Indiana University Low Energy Neutron Source: Applications to the Study of Nanostructed Materials*. ProQuest LLC, Ann Arbor, MI (2007).

[12] Shin, T., Findenegg, G.H., and Brandt, A. *Surfactant Adsorption in Ordered Mesoporous Silica Studied by SANS.* In Progr. Colloid Polym. Sci. (2006).